THE 2.8 Å CRYSTAL STRUCTURE OF A CONSTITUTIVELY ACTIVE ALPHA TRANSDUCIN SUBUNIT

A Thesis

Presented to the Faculty of the Graduate School

of Cornell University

In Partial Fulfillment of the Requirements for the Degree of

Master of Science

by

Eric C Hillpot

August 2019

ABSTRACT

G protein coupled receptors play important roles in cellular signaling and are stimulated by a multitude of extracellular signals. These proteins initiate signal transduction cascades that elicit a variety of cellular responses. Once activated, G protein coupled receptors activate G proteins which further stimulate target proteins to elicit cellular responses such as enzyme activity, translation and ion channels[60]. In this study, we set out to solve the crystal structure of a constitutively active form of the alpha subunit of the retinal G protein, transducin. This activated G protein, designated as α_T* SFD QLRC, elicits the ability to stimulate its effector molecule, PDE, to levels comparable to activated native retinal alpha. Crystals of α_T* SFD QLRC were grown and x-ray diffraction data sets were observed at low resolution. Following insights from a recent paper by Hu *et al*, 2018, a C210S mutant was created to help improve diffraction. Data sets of α_T* SFD QLRC C210S were collected to 2.8 Å and compared to previously solved GDP-bound (1TAG) and GTPγS-bound (1TND) native α_T subunits. The crystal structure of α_T* SFD QLRC C210S reveals that despite being fully active *in vitro*, GDP, and not GTP, is bound in the structure. As a result, Switch II and Switch III appear to be in a transition state between the inactive GDP-bound state and the active GTP-bound state and are un-modelled due to low electron density. Future work involves improving crystallization of α_T* SFD QLRC C210S to obtain a GTP-bound structure so that the structure can be used to elucidate the mechanism by which the transducin α subunit, especially the phenylalanine residue of the SFD mutation, confers maximum PDE activity.

BIOGRAPHICAL SKETCH

Eric Hillpot is a graduate student from Pennellville, New York. He graduated from Clarkson University in May of 2018 with his Bachelors of Science majoring in Biology and minoring in Chemistry.

ACKNOWLEDGEMENTS

I would like to extend my warmest thanks to those to whom without, I would never have succeeded.

- Shawn K. Milano for being a great mentor and friend for my time at Cornell University
- Richard A. Cerione for being a great mentor and providing me with the opportunity to study under him
- My loving parents for supporting and encouraging me throughout my college years

TABLE OF CONTENTS

INTRODUCTION

Vertebrates have developed specialized organs known as the eye to maximize light stimulation[1,2]. The eye consists of a membranous lens which captures light from the environment and focuses this light at the back of the eye. Nerve cells at the back of the eye known as the retina absorb this light and pass information to the optic nerve and brain. To do this, the retina contains specialized nerve cells known as rods and cones. Rods and cones absorb light and transmit a chemical signal to the brain which we perceive as an image[3]. What are the underlying biochemical processes that allows us to see the world in front of us? After all, light is simply a photon striking our eyes.

The prototypical signaling cascade of G protein-coupled receptors (GPCRs) involves a transmembrane receptor, a guanosine nucleotide-binding (G) protein and an effector molecule. The transmembrane receptor surveys the extracellular environment for signals. Once a stimulant binds to the receptor, structural changes within the receptor activates the G protein. Once activated, the G protein will undergo structural changes and stimulate effector molecules which change the intracellular concentrations of secondary metabolites or other important signaling molecules. This cascade of events causes transcriptional, translational or other changes within the cell in response to the stimuli. There are various GPCRs, G proteins and effector molecules in the cell but all follow the similar pathway shown below (Figure 1). In the vision system, the GPCR is rhodopsin, the G protein is transducin and the effector protein is cGMP phosphodiesterase (PDE). The visual phototransduction system is a prototypical GPCR

signaling cascade. In this study, we focus on this pathway and the key proteins involved.

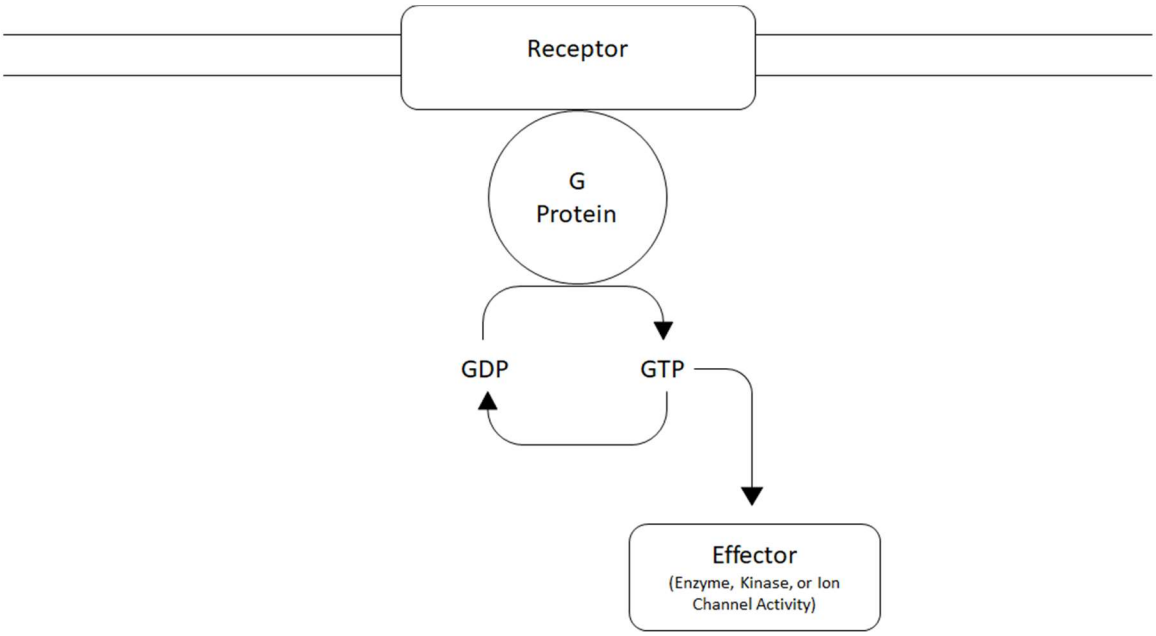

Figure 1: The canonical GPCR Signaling pathway within cells.

Rhodopsin is a member of the superfamily of GPCRs. GPCRs constitute the largest family of transmembrane proteins in metazoan biology consisting of about 800 members[4] and are targeted by over 30% of all drugs[5] on the market. All GPCRs share the characteristic seven transmembrane helices and transmit extracellular signals from a wide array of signals including; hormones, neurotransmitters, odorants and photons[6]. GPCRs transmit these signals across the plasma membrane and allow cells to survey the surrounding environment and respond accordingly.

In humans, each retina contains nearly 10^9 rod cells which are more sensitive to light but cannot distinguish color and $3x10^6$ cone cells which are less sensitive to light

but can distinguish color[7]. This explains why it is difficult to see color in dim light. Rod and cone nerve cells each contain the light-sensitive receptor protein, rhodopsin. Native rhodopsin has been purified from bovine eye and used in experimentation to better understand GPCR and G protein signaling. To learn more about GPCR signaling, crystal structures must be obtained to help identify important G protein binding sites. Eventually, the three dimensional crystal structure of detergent-solubilized bovine rhodopsin was first reported at 2.8 Å resolution[8] and recently improved to 2.2 Å[9]. These inactive structures show that rhodopsin folds into a seven transmembrane helix which is characteristic among GPCRs.

Rhodopsin is comprised of the ~40kDa protein component, opsin, bound to the chromophore moiety, 11-cis-retinal. 11-cis-retinal is bound to opsin[10, 55] via a Schiff base linkage to the ε-amine of lysine 296 in the middle of transmembrane helix 7[10]. This covalently bound inverse agonist, 11-cis retinal, photoisomerizes into all-trans retinal which becomes an agonist for rhodopsin upon light-activation[11, 57] . The photo-induced change in the structure of rhodopsin results in the creation of a binding site along the cytosolic helix for the G protein, transducin[4]. Closely related GPCR and G protein complexes have been crystallized and their structures determined.[12, 13, 14, 15]. Additionally, cryo-electron microscopy has been recently used in the lab by Dr. Gao to solve the structure of the rhodopsin-transducin complex[61]. These structures depict the binding interactions between the GPCR and G protein. The vertebrate vision system was the first GPCR signaling pathway in which each component has been purified and crystallized and provides a good example to study a multi-component, GPCR-G protein-coupled signaling system[16].

In the active structure, the transmembrane helices of rhodopsin move which ultimately result in key changes within the cytosolic region of the receptor[17,18]. Once 11-cis retinal absorbs a photon and changes conformation to all-trans-retinal it causes structural changes generating the active receptor form known as metarhodopsin II[19]. Metarhodopsin II activates transducin via contacts of the cytosolic helix of the receptor and Domain III, the carboxy terminus, of the α subunit of transducin[20]. Once activated by light, metarhodopsin II binds and catalyzes the exchange of GDP for GTP within the α subunit of the heterotrimeric G protein, transducin[21].

The next step in GPCR signal transduction is G protein activation. In the phototransduction cascade, the G protein is transducin. There are two families of G proteins, the Ras-related single chain (small) G proteins and the heterotrimeric (large) G proteins. Here, we will focus on heterotrimeric G proteins, of which transducin is a member. G proteins interact with various effectors within the cell which have diverse cellular consequences regulating enzymes, ion channels, transporter proteins and other parts of the cell machinery controlling motility, transcription, secretion and contractility[60]. G proteins function as molecular switches, therefore their signaling regulation is important to prevent excessive signaling which can be detrimental to an organism's health. In the canonical pathway, GPCRs activate G proteins through GTP/GDP exchange while regulator of G protein signaling (RGS) proteins help inactivate G proteins by promoting GTP hydrolysis by the α subunit of G-proteins[22]. The activity of G proteins depends on whether GDP or GTP is bound within the α subunit. G proteins are activated upon GTP binding and inactivated once GTP is hydrolyzed to GDP[58]. There are various α subunits which activate or inhibit effectors.

In contrast to the great diversity of GPCRs (800 members), there are only 16 genes encoding 21 different α subunits in humans[23]. This implies that each G protein isoform must interact with several different GPCRs. Notably, there is evidence supporting that GPCRs, such as the $ß_2$ adrenergic receptor, can couple to more than one G protein[24]. Therefore, proper regulation regarding the specificity between GPCRs and G proteins is imperative for normal signal transduction within cells[25]. Improper signaling causes aberrant intracellular responses which can cause the onset of diseases at the organismal level such as cancer[26, 53]. Therefore, it is important to fully understand these signaling pathways and to develop new treatments and medicines when these pathways are disrupted.

In their inactive basal state G proteins are bound to GDP, however following activation of the GPCR via a hormone or other type of signal, GDP dissociates and is replaced by cellular GTP. In humans, the intracellular concentration of GTP is about ten-fold higher than GDP, therefore GTP is more likely to be exchanged than GDP[27]. The binding of GTP causes a conformational change within the G protein which then primes it to interact with the next protein in the signaling pathway such as its target or effector protein. GTP hydrolysis by the G protein then returns it to its inactive GDP-bound state. A summary of this process is shown below (Figure 2).

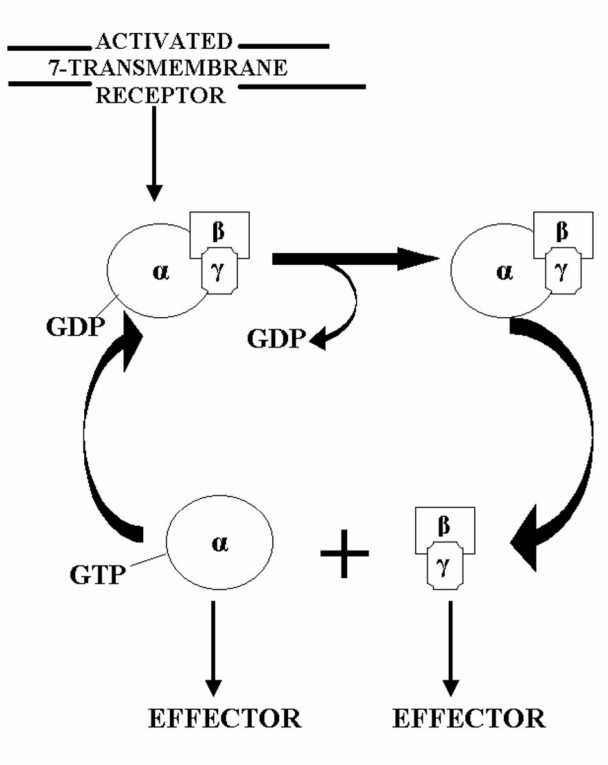

Figure 2: G proteins as molecular switches. Figure depicting the regulatory cycle of heterotrimeric G protein subunits[28].

To send intracellular signals, GPCRs activate their canonical signaling partners, large heterotrimeric G proteins. Large heterotrimeric G proteins are comprised of α, ß and γ subunits which are ~40-45 kDa, ~35-36 kDa and ~5-10 kDa respectively[29]. Small, Ras-like G proteins are a single chain which is ~21 kDa. Gα subunits contain two domains, a domain involved in binding and hydrolyzing GTP (sometimes referred to as the G domain or the Ras-like GTPase domain) and a unique helical domain that buries GDP or GTP within the core of the protein. The guanine nucleotide-binding, or G, domain is highly conserved in G proteins. The ß subunits of large G proteins have a seven-membered ß-propeller structure as indicated by the presence of seven WD40 (tryptophan-aspartic acid) repeats. ß and γ subunits form a functional unit that is not

dissociable except by denaturation and function as regulators of the α subunit. ß and γ subunits can also function as separate signaling proteins and activate other second messengers or by gating ion channels directly[30, 31]. There are four different types of heterotrimeric G proteins based on the amino acid sequence similarity of the α subunits: G_s, G_i, G_q, and G_{12} and each vary in activity with effectors[32, 41, 42, 43]..

The first three dimensional structure of a G protein-α subunit solved was of transducin. It was solved in an activated conformation (GTPγS-bound) by Sigler and his colleagues, and was considered to represent a remarkable breakthrough at the time[33]. This original X-ray crystal structure showed that bound GTPγS, a non-hydrolysable GTP analog, molecule was occluded in a deep cleft between a domain structurally homologous to Ras and a helical domain unique to heterotrimeric G proteins. The Ras-like and the helical domain of G protein-α subunits in effect form a “clam shell” that seals the bound GTP. This has significant consequences for the mechanism by which GPCRs stimulate GDP-GTP exchange and catalyze G protein activation. Metarhodopsin II must pry open the “clam shell” to allow GDP to dissociate and allow GTP to associate before closing tightly. A number of structures rapidly followed for GDP-α_T[34], GDP[35] and GTPγS[33]-bound α_{i1}, and the α_T-ßγ (holo-transducin)[34] and α_{i1}-ßγ (holo-G_{i1})[29] complexes. When the structure for the GDP-bound α_T subunit was solved, it was possible to overlay and compare the structures for an activated and an inactive a subunit. This provided key insights into the molecular consequences and structural changes of G protein activation that accompanies GTP/GDP exchange.

Stimulated rhodopsin induces structural changes within transducin which catalyzes GTP/GDP exchange[56]. Structural changes within the α subunit induced by GTP/GDP exchange are localized to three adjacent regions on one face of the protein. These regions are referred to as Switch I, II and III due to their essential movement in activation. Switch I (Ser173-Thr183) and Switch II (Phe195-Thr215) have counterparts in Ras. However, Switch III (Asp227- Arg238) is unique to heterotrimeric G proteins. The major helical domain on α_T is largely unchanged by GTP/GDP exchange as is the α4-ß5 region. The GTP-bound α subunit of transducin, α_T, dissociates from the ß and γ subunits and can then interact with and activate its effector molecule, PDE, which hydrolyzes cGMP to GMP and with the release of a proton.

The crystal structure for holo-transducin was solved and showed two non-overlapping regions of contact between the α and ß subunits, an extended interface between ß and nearly all of γ, and a limited interaction between the α and γ subunits[34]. A major binding interaction between the G_α and $G_ß$ subunits involves the Switch II domain of the α subunit, with the GTP-bound structural rearrangement of Switch II being responsible for the dissociation of the G_α subunit from the $G_{ßγ}$ complex allowing G_α to activate PDE[36, 37]. A second major contact between the G_α and $G_ß$ subunits occurs within the amino terminal domain of α. WD40 repeats that are found in the $G_ß$ subunit show up in a variety of other proteins involved in signaling, RNA processing, gene regulation, vesicle fusion, and cytoskeletal assembly. These WD40 repeats form a circularized seven-fold ß propeller. The N-terminus of $G_ß$ adopts an α-helical conformation that forms a coiled-coil motif with the N-terminus of $G_γ$. The C-terminus of $G_γ$ binds to blades five and six of the seven-bladed ß-propeller structure. The primary

interaction surface between the G_α and $G_ß$ subunits is formed by Switch I and Switch II on G_α(GDP) and five of the seven blades of $G_ß$. A smaller interaction is formed between the N-terminus of G_α and blade one of $G_ß$. Upon formation of the heterotrimer, $G_{ßγ}$ significantly alters the conformation of Switch I and Switch II, which dismantles the binding sites for Mg^{2+} and the γ-phosphate of GTP, consistent with the notion that GTP and $G_{ßγ}$ binding to G_α are negatively cooperative.

The final step of the GPCR signaling cascade is effector activation (PDE6 in the visual system). Regulation of this signaling cascade has serious implications in diseases such as cancer. In the visual transduction signaling pathways, activated GTP-bound transducin relieves the inhibitory γ subunit of PDE6 to activate it (the precise mechanism is not yet known). Once activated, PDE catalyzes the hydrolysis of cGMP to GMP. In neuronal cells, cGMP binds to and opens sodium ion channels in photoreceptors allowing sodium cations to freely diffuse into the cell from the extracellular environment. However, once cGMP is converted to GMP, the sodium ion channels close which prevent cations such as Na^+ and Ca^{2+} from entering the cell. Simultaneously, Na^+ is transported out of the neuronal cell by another ion channel, Na^+K^+ ATPase[38]. The result is Na^+ being net exported from the cell which will hyperpolarize the cell and generate an electrical action potential which transmits the stimulus of light to the brain. This is the final step of the vision signal transduction cascade[54].

The rhodopsin phototransduction signaling pathway is the paradigm for GPCR and G protein signaling. The system offers certain advantages when compared to other

GPCR signaling pathway for obtaining structural insights into GPCR-signaling. Most importantly, each of the principal components of the pathway can be purified from native tissue in large quantities. As a result, rhodopsin was the first and only GPCR to date for which X-ray crystal structures have been solved in native form. While this serves as a great advantage over other GPCR signaling pathways, there is one major drawback. To better understand critical residues which are paramount for protein-protein interactions and function, point mutations must be introduced into the protein. In doing so, critical residues for ligand binding, activity, protein-protein interaction, specificity, and regulation, can then be elucidated despite large quantities of phototransduction proteins readily purified from bovine eye, these proteins are native and cannot be mutated. Therefore, it would be highly desirable to reconstitute and express phototransduction proteins within a bacterial model because bacteria can be genetically manipulated.

Each of the primary components of the rhodopsin/transducin-coupled signaling pathway has been purified, biochemically characterized, and their interactions reconstituted *in vitro*. This system is ideal for elucidating the underlying mechanisms that link the GTP-dependent interactions between a G_{α} subunit and its biological effector. However, to study key sites on G_{α} subunits for effector regulation, targeted mutagenesis followed by bacterial expression must be utilized. α_T has previously been unsuccessfully expressed in *Escherichia coli* and thus could not be mutated for further studies until a paper published by Skiba *et al*. In this paper, the researchers spliced together two DNA sequences from α_T and $G_{\alpha i1}$, forming various chimera proteins, one variant was designated α_T Chi8. This chimera could be expressed in bacteria[39]. α_T Chi8 is composed of two fragments of α_T, residues 216–227 and 237–294, which were

replaced with the corresponding residues from another G protein, α_{il}. The *E. coli*–expressed α_T Chi8 chimera has greatly facilitated biochemical and crystallographic structural studies and expanded the study of G proteins. Despite these great advances, α_T Chi8, could not stimulate its effector, PDE, to any degree. Further investigation revealed that restoration of two residues in the α3 helix of α_T (His-244 and Asn-247: HN mutant) yielded partial restored PDE activation; α_T Chi8 HN. A recent study by Milano *et al.* was able to fully reconstitute PDE effector activity through α_T Chi8 HN after further mutagenesis. This was achieved through mutating three residues of α_T Chi8 HN which restored the αG/α4 loop from α_T[40]. This fully active chimera, α_T Chi8 HN SFD (from here referred to as α_T* SFD), could fully stimulate PDE, after GTP/GDP exchange, to levels comparable to native transducin from bovine eye. Importantly, further analysis identified the critical Phe-283 residue that is essential for conferring maximum stimulatory capability upon the retinal G_α subunit. This study aims to highlight the importance of these key residues of Gα sites in mediating effector regulation.

Here, we show that further mutagenesis of α_T* SFD to α_T Chi8 HN SFD QLRC (from here referred to as α_T* SFD QLRC) formed a constitutively active α_T subunit without the need for GTP/GDP exchange. The QLRC mutations (Q200L and R174C) removed critical residues for GTP hydrolysis within α_T and reduced the intrinsic GTP hydrolytic activity. This study aims to crystallize α_T* SFD QLRC to observe the active conformation and gain structural insight of how this α_T subunit recovers full PDE activity.

MATERIALS AND METHODS

Site-directed Mutagenesis

Sense and antisense oligonucleotide primers were synthesized with the sequence including the desired mutated base in the center of the primer. The QuikChange site-directed mutagenesis kit (Stratagene) was used for PCR-based mutagenesis on miniprep plasmid DNA. The parental DNA template was digested using DpnI endonuclease and the nicked vector DNA with the desired mutation was transformed into NEB 5-alpha supercompetent cells. A chimeric α_T construct, referred to as α_T Chi8, was obtained from Dr. Heidi Hamm's laboratory at Vanderbilt University. This chimera was generated by substituting two regions of α_{i1} (residues 216–227 and 237–294) for the corresponding residues of native retinal α_T to facilitate its expression in *E. coli.* A modified chimera was created by mutating residues K244H and D247N in α_T-Chi8, resulting in a chimeric G subunit referred to as HN. Further mutation of residues yielded the α_T Chi8 HN SFD QLRC mutant which was later expressed in BL21 (DE3) supercompetent cells, purified and crystallized.

*Expression and purification of α_T*SFD QLRC*

BL21 cells were transformed by incubating 1µg of DNA with bacteria on ice for 15 minutes. The bacteria were then heat shocked at 45^{o}C for 30 seconds before being placed immediately back on ice. Transformed bacteria were grown for 1 hour in a 37^{o}C shaker incubator in SOC growth media. Transformed bacteria were placed on lysogeny broth (LB)-Agar-ampicillin plates to select for colonies overnight. Single colonies were

picked after an overnight incubation at 37°C and bacteria were cultured overnight in a 125 mL starter culture containing LB with 100 mg/L ampicillin at 37°C on a shaker. Bacteria were then cultured in 1L flasks containing autoclaved media consisting of 12 g/L tryptone, 24 g/L yeast extract, 4 mL pure glycine, 2.3 g/L KH_2PO_4, 12.5 g/L K_2HPO_4 and 100 mg/L ampicillin. Cultures were grown for 3-6 hours in a 37°C table shaker until an optical density of 0.6 - 0.8 was reached. 30 µM IPTG was added to induce plasmid expression overnight at 23°C on a table shaker. Cultures were then centrifuged for 10 minutes at 5000 rpm at 4°C using a JLA 10.500 rotor (Beckman Coulter) and an Avanti J-25I centrifuge (Beckman Coulter). Bacteria pellets were collected and stored at -20°C until further use. Bacteria were lysed using lysis buffer consisting of 50mM Tris, 50mM NaCl, 5mM $MgCl_2$, 5 mM ß-mercaptoethanol, 1mM GDP, and 0.1 mM PMSF using an ultrasonic converter connected to a 550 sonic dismembrator (Fisher Scientific) sonicator on ice. Bacteria lysates were centrifuged for 45 minutes at 40,000 g at 4°C under vacuum using a TI45 rotor and Optima LE-80K ultracentrifuge Beckman Coulter ultracentrifuge. Bacterial lysis supernatant was passed over a sepharose column charged with 250 mM $NiSO_4$. Supernatant was incubated with the charged nickel column for 5 minutes at 4°C before starting elution. Stepwise elution followed with three buffers and fractions were collected once the third buffer was added. Nickel column buffer 1 consisted of 50 mM Tris pH 8.0, 500 mM NaCl, 20 mM imidazole, 50 µM GDP and 5 mM ß-mercaptoethanol. Nickel column buffer 2 consisted of 50 mM Tris pH 8.0, 20 mM imidazole, 50 µM GDP and 5 mM ß-mercaptoethanol. Nickel affinity column buffer 3 consisted of 50 mM Tris pH 8.0, 500 mM NaCl, 100 mM imidazole, 50 µM GDP and 5 mM ß-mercaptoethanol. The proteins were further purified by ion exchange

chromatography using a HiTrap Q FF Sepharose column (GE Healthcare Life Sciences) using a buffer containing 50 mM Tris pH 8.0, 5 mM $MgCl_2$, 1 mM DTT, 10% glycerol, 25 μM GDP and a linear concentration gradient of NaCl from 20 mM to 1 M. 5 mL fractions were collected until 15 fractions were collected and then 2 mL fractions were collected to improve elution resolution. The chromatography peaks containing α_T Chi8 HN SFD QLRC were pooled and passed through a HiLoad Superdex 75 gel filtration column (GE Healthcare) size exclusion chromatography column using a buffer containing 20 mM Na-HEPES pH 7.5, 5 mM $MgCl_2$, 100 mM NaCl, 10% glycerol and 1 mM DTT. All purification buffers were filtered using a nylon membrane 0.20 μm GNWP filter (Merck Millipore Ltd.). Fractions containing α_T Chi8 HN SFD QLRC were pooled and concentrated if necessary to 10 mg/mL using Ultracel 10K centrifugal filters (Amicon) and snap frozen and stored at -80°C. Protein concentrations were determined by using absorbance at 280 nm and the calculated molar extinction coefficient. The molar extinction coefficient was calculated from their sequence using the ExPASy ProtParam tool (https://web.expasy.org/protparam/). To verify protein purity, samples were run on a Novex WedgeWell 4-20% Tris-glycine gel (Invitrogen) alongside a Precision Plus Protein Standard (BioRad). The gel was then stained for all proteins using Coomassie Blue fast stain (Gene Copoeia). Rhodopsin was purified as described here[16].

Crystallization

Purified α_T* SFD QLRC was concentrated to 10 mg/mL and screened under many conditions using the Gryphon (Art Robbins Instruments). Several 96 well screens from Hampton Research were used to find conditions that promoted crystallization.

Screens included Index, 50% compass, SaltRx, Grid Screen Salt and Crystal screen (Hampton Research). Once initial crystal conditions were identified, finer screens in 24 well plates were set up to optimize crystal growth, size, quality and quantity. Hanging drop vapor diffusion was used for crystal growth under conditions consisting of 2.4 M $(NH_4)_2SO_4$ and 0.1 M sodium cacodylate pH 6.0. Crystals were then picked using nylon magnetic loops (Hampton Research) and flash frozen in liquid nitrogen with 3.2 M $(NH_4)_2SO_4$ and 0.1 M sodium cacodylate cryoprotectant and stored in liquid nitrogen until diffracted at the Cornell High Energy Synchrotron Source (CHESS) at Cornell University, Ithaca, NY. Diffraction images were collected on the F2 beamline. All components used for crystallization solutions were acquired through Hampton Research.

Structure Determination

At CHESS, diffraction images were collected on the F2 beamline. Diffraction images were collected while the crystal diffracted under a cryo stream. HKL2000 (HKL Research Inc)[44] was used to determine the space group and integrate the images into an MTZ file. Python-Based Hierarchical ENvironment for Integrated Xtallography version (PHENIX)[45] was used for molecular replacement using the 1TND (GTPγS-bound) pdb model to solve the structure. PHENIX and coot[52] were used to refine the three-dimensional structure within the electron density. Several rounds of refinement were used to optimize integration in PHENIX.

Purification of retinal proteins

The exact procedure was followed from Milano *et al*[40]. Bovine rod outer segment membranes were isolated using a sucrose gradient as described previously[46]. Urea-washed disc membranes were prepared as described and served as the source of light-activated rhodopsin[47]. PDE and transducin were isolated by washing rod outer segment membranes with hypotonic buffer in the absence and presence of GTP. The α_T subunit and $ß_1\gamma_1$ subunit complex of transducin were resolved on a HiTrap Blue Sepharose column (GE Healthcare). The column was first washed with a buffer containing 10 mM NaHEPES, pH 7.5, 6 mM MgCl2,1mM DTT, 100 mM KCl, and 10% glycerol to elute the $ß_1\gamma_1$ complex. To elute α_T, a buffer containing 10 mM Na-HEPES, pH 7.5, 6 mM MgCl2, 1mM DTT, 500 mM KCl, and 10% glycerol was subsequently applied onto the column. All transducin subunits and holo-PDE were loaded on HiLoad Superdex 75 and Superdex 200 gel filtration columns (GE Healthcare), respectively, and eluted with a buffer containing 20 mM Na-HEPES, pH 7.4, 5 mM MgCl2, 100 mM NaCl, and 1 mM DTT. The pure retinal proteins were concentrated to 20 µM, snap frozen, and stored at 80°C.

PDE Effector pH Assay

PDE activity was measured through cGMP hydrolysis and determined by the change in buffer capacity over time. 200 µL of reaction buffer containing 10 mM Tris pH 8.0, 2 mM $MgCl_2$ and 100 mM NaCl and GTPγS-loaded α_T subunits, at varying concentrations, were incubated with either holo-PDE or reconstituted PDE (50 nM) in a 96 well plate. The pH (in millivolts) was monitored in real time and once a stable

baseline was achieved, 5 mM cGMP was added and the decrease in pH was recorded for 150 s. The buffer capacity of the mixture was then determined by adding NaOH (400 nmol). The hydrolysis rate of cGMP (nmol/s) was determined from the ratio of the initial slope of the ph record from cGMP hydrolysis (mV/s) and the buffer capacity of the assay buffer (mV/nmol).

RESULTS

Purification of α_T Chimeras

Previous studies have purified α_T chimeras from bacterial systems using similar methods. The construct of these α_T chimeras have a C-terminus 6 repeat histidine tag as histidine residues have high affinity for nickel and strongly coordinate with nickel ions bound to the stationary phase in the column. Genetically engineering a His-tag into the protein constructs allows for separation of α_T from the majority of other proteins within the *E. coli* cells via affinity chromatography. Imidazole is used for elution and as its six pi-electrons coordinate nickel more strongly than does histidine. As increasing concentrations of imidazole are added to the column, first the more weakly associated proteins lacking any His-tag elute. Only in the third buffer, and at the highest imidazole concentration, is the His-tag protein eluted and collected for further purification.

The next step of purification is ion-exchange chromatography where separation is based on the reversible interaction between a charged protein and an oppositely charged chromatography resin. Increasing concentrations of NaCl are used to elute proteins from the ion-exchange column. Fractions containing the highest α_T concentration are pooled together and run over the gel-filtration column. This column consists of the stationary phase in which the beads have tunnels of pores that run through the interior of the bead. Small sized proteins interact with these pores more than do larger proteins which cannot fit into these pores and thus larger proteins elute faster than small proteins. This is the final step in purification and selects for a ~40kDa

protein, α_T* SFD QLRC (Figure 3). The coomassie gel was overloaded with 20 µg of purified α_T to reveal contaminant co-purified proteins. Co-purified proteins are likely to associate with α_T and evade the series of chromatography columns. The purity of protein strongly influences its ability to form highly diffracting crystals.

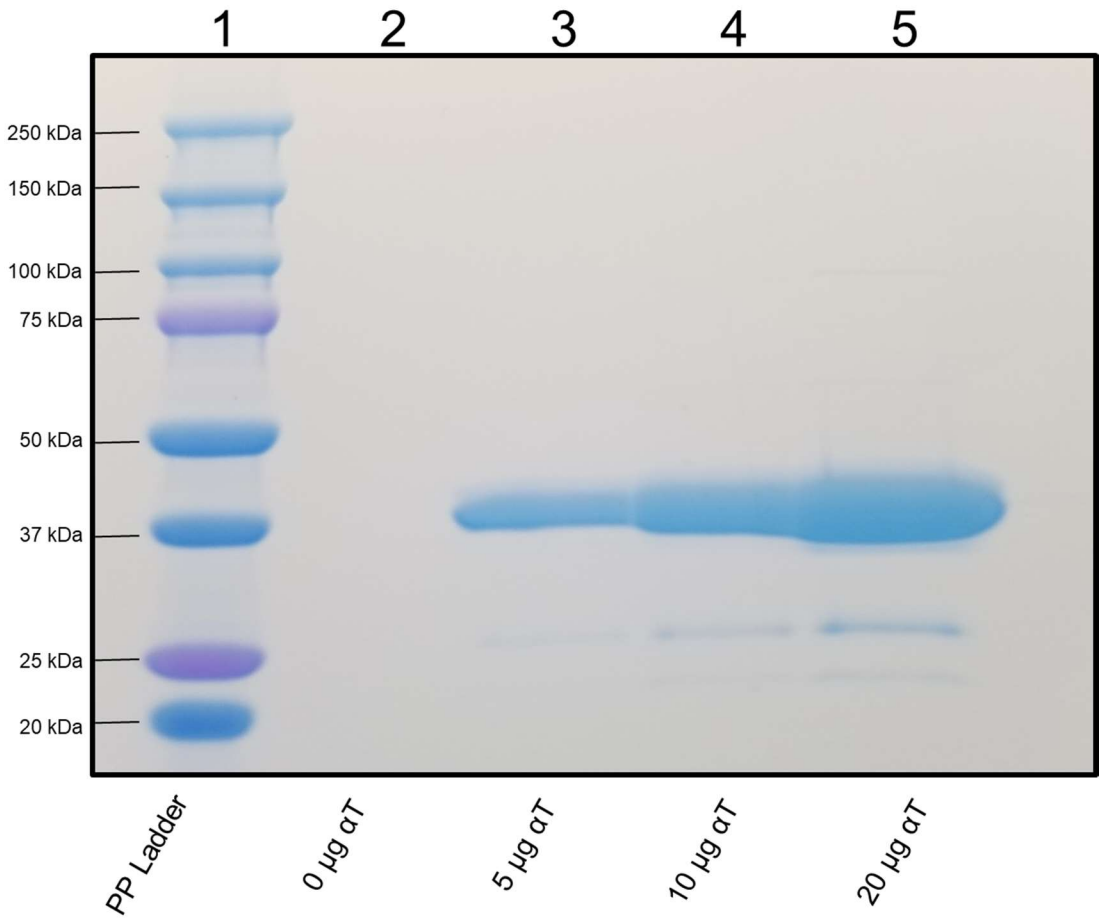

Figure 3: Purification of α_T* SFD QLRC. Coomassie stained gel of the purified α subunit of transducin. Precision Plus Protein Standard (BioRad) was loaded into lane 1 and served as a marker for protein molecular weight. Lanes 2 through 5 were added with 0, 5, 10 and 20 µg of purified αT. The gel was stained with Coomassie Blue fast stain (Gene Copoeia) and destained overnight. Proteins retain the coomassie stain and are seen as horizontal blue bands. The dark blue band at ~40 kDa represents purified α_T* SFD QLRC.

α_T SFD QLRC effector activity*

The immediate biological effector of α_T is PDE. The first step after purifying α_T was to access its ability to activate PDE. Once rhodopsin catalyzes the exchange of GDP for GTP within the GTPase domain of α_T, the ß and γ subunits dissociate. α_T dissociates from rhodopsin and binds to and activates PDE by relieving the inhibitory γ subunit[47]. Once activated, PDE hydrolyzes the cyclic phosphodiester bond bound to the 3' hydroxyl group of deoxyribose of guanosine. 5'-GMP and a proton are generated as products. Therefore, by monitoring the change in pH as a function of buffer capacity, the ability of α_T to activate PDE can be measured. Previous experiments, by Milano *et al* 2018, showed that the SFD mutant was GDP-bound and must be exchanged with GTP using rhodopsin, ß and γ subunits of transducin as well as light. In doing so, the activity of SFD increased to levels comparable to retinal α. Without GTP exchange, SFD showed minimal activity, similar to GDP-bound retinal α. These data show that the SFD mutant is normally bound to GDP and must be exchanged to GTP to become active. However, the α_T* SFD QLRC mutant showed maximal activity without rhodopsin-catalyzed exchange. These results suggest that α_T* SFD QLRC either is bound to GTP or constitutively in an active conformation and able to activate PDE (Figure 2). HPLC data using elution absorbance peaks of GDP and GTP reveal that α_T* SFD QLRC elutes mainly with GTP and a minor population with GDP (data not shown). This suggests that α_T* SFD QLRC binds to GTP in favor of GDP. Site-directed mutagenesis was performed to create the α_T* SFD QLRC mutations which have been shown previously to reduce GTP hydrolysis within the GTPase domain of α subunits[48]. Therefore, once α_T* SFD QLRC binds to GTP, it will be in an active conformation. Our

results are consistent with these previous findings. However, to prove this, the crystal structure of α_T* SFD QLRC must be solved.

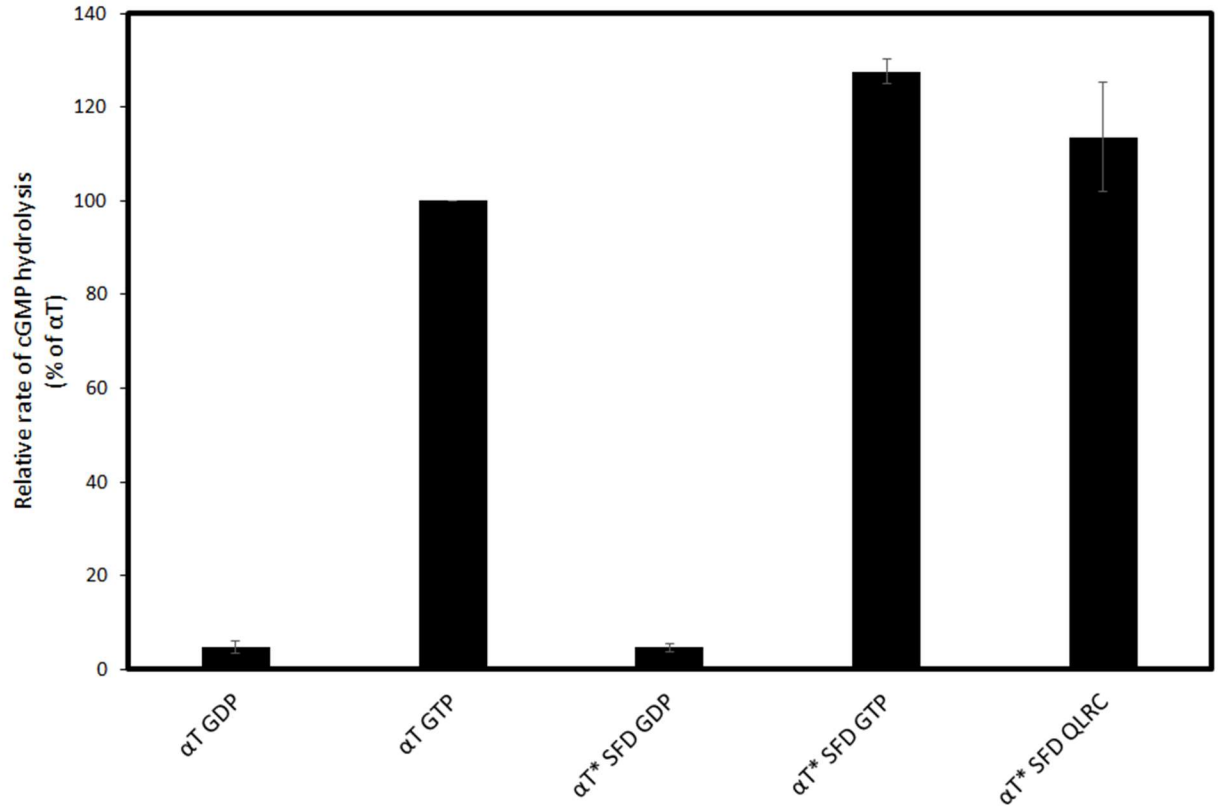

Figure 4: α_T* SFD QLRC effector activity. PDE stimulation by α_T subunits. The activity of PDE as monitored by pH and graphed as the relative rate of cGMP hydrolysis. Retinal α from bovine eye were purified, α_T SFD and α_T SFD QLRC from *E. coli* were purified and were assayed for activity. Only retinal alpha and SFD were exchanged with GTP using activated rhodopsin. The concentration of the α_T subunits used in this experiment was 1μM. The percent rates of cGMP hydrolysis of the α_T subunits were plotted relative to the levels of cGMP hydrolysis stimulated by native retinal α_T. Data is represented as a mean with ± S.E.(error bars) of at least three replicates.

Structure Determination of α_T SFD QLRC C210S*

Initially, α_T* SFD QLRC crystal trays were set up. Crystals formed but diffracted weakly. However, a recently published paper revealed that creating cysteine mutations within an α_s subunit of a G protein helps promote crystallization in the active

conformation[4]. To help improve crystal diffraction, a similar mutant of α_T was made. The final protein construct is now noted as α_T* SFD QLRC C210S.

α_T* SFD QLRC C210S crystals were grown (as shown below in Figure 5A) and diffracted to 2.8 Å. Diffraction images from CHESS are shown (Figure 5B) and a summary of crystal statistics is tabled (Figure 5C). The crystal structure was solved to 2.8 Å and is shown below (Figure 5D and E). The overall structure is shown in gray and the three Switch regions are colored. Switch I is colored in red, Switch II in blue and Switch III in purple. The helical domain, GTPase domain, effector binding domain and receptor binding domain are shown. The structure contains GDP as shown in green. The model is shown in cartoon format to reveal secondary structures except for switch regions shown as sticks for clarity.

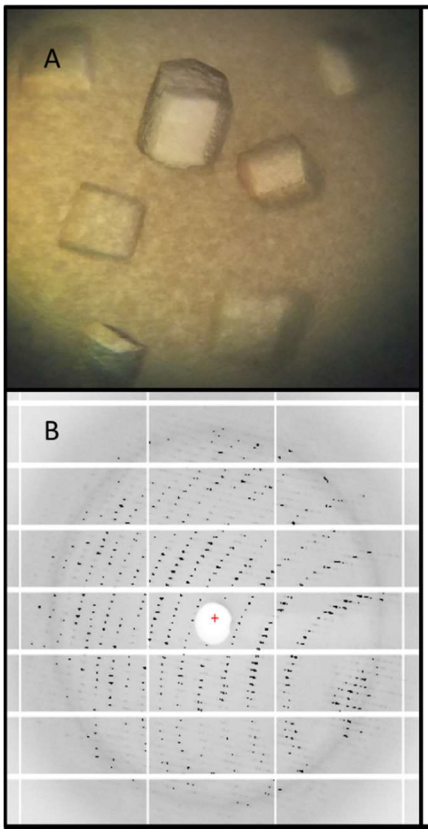

C **Data collection and refinement statistics (Molecular Replacement)**

	α_T Chi8 HN SFD QLRC C210S
Data collection	
Space group	P 43 21 2
Cell dimensions	
a, *b*, *c* (Å)	94.313, 94.313, 385.255
α, β, γ (°)	90, 90, 90
$I / \sigma I$	13.1 (42.3)
Completeness (%)	100 (99.9)
Redundancy	12.9 (13.4)
Refinement	
Resolution (Å)	24.781-2.802
R_{work} / R_{free}	0.2247 / 0.2802
R.m.s. deviations	
Bond lengths (Å)	0.010
Bond angles (°)	1.193

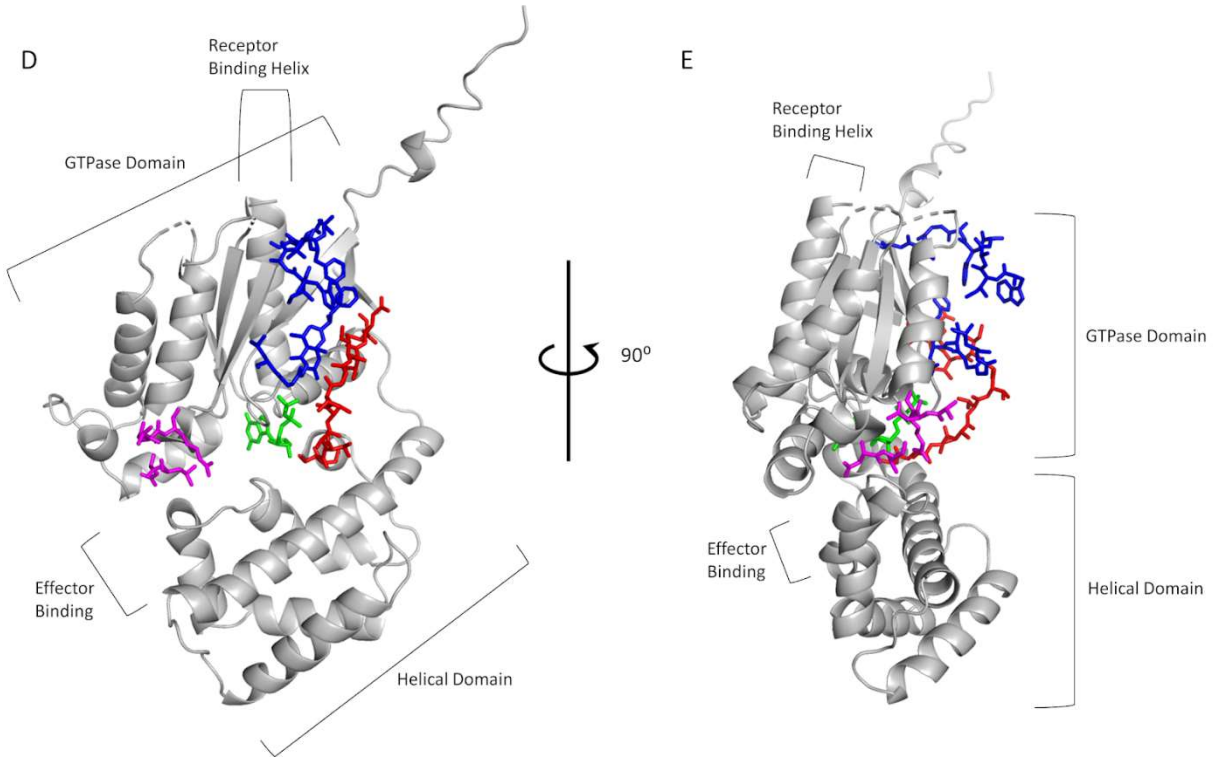

Figure 5: Diffraction and structure of α_T* SFD QLRC C210S crystals: Crystallized α_T* SFD QLRC C210S diffracted to 2.8 Å. A. crystals seen under the microscope in the hanging drop vapor diffusion tray. B. diffraction image of the crystals at CHESS. C. summary of crystallographic diffraction statistics and refinement. Diffraction images were indexed and integrated using HKL2000. Phenix and coot were used for 3d modelling and refinement. D and E. the 3d crystal structure solved to 2.8 Å. The overall structure (gray) with GDP bound (green) and the three Switch regions, I (red), II (blue) and III (purple). The structure is shown in cartoon style to highlight secondary structures while GDP and the Switch regions are shown in stick style. The important regions of α_T are depicted as extended brackets and labels. The protein is viewed from two angles: 0 degrees (D) and 90 degrees (E). Images were created using PyMOL.

Comparison of α_T SFD QLRC C210S to native α_T GDP and GTPγS structures*

Interestingly, the mutant protein shows full ability to activate its effector, PDE, but is somehow bound to GDP instead of GTP. Therefore, the crystal structure was aligned with other retinal α_T crystal structures either bound to GDP or GTPγS (Figure 6). The α_T* SFD QLRC C210S structure (green) was aligned with both the GDP-bound

structure, 1TAG (purple) and the GTPγS-bound structure, 1TND (yellow). Images were created using the same alignments and field of view in PyMOL[49]. Overall, the global structures of the three proteins are highly similar. Because the α_T* SFD QLRC C201S structure showed density for GDP, we compared the guanosine-binding pocket of α_T* SFD QLRC C201S to both GDP-bound and GTPγS-bound structures. The aligned structures show strong similarity in the binding pocket to one another. The only notable difference seen is in the GTPγS-bound structure where GLY-199 moves to form a hydrogen bond with the γ-phosphate of GTPγS so as to accommodate the additional phosphate. Also, in the GTPγS-bound structure there is a Mg^{2+} cation that coordinates with oxygen atoms from both the ß and γ-phosphate of GTPγS (not shown).

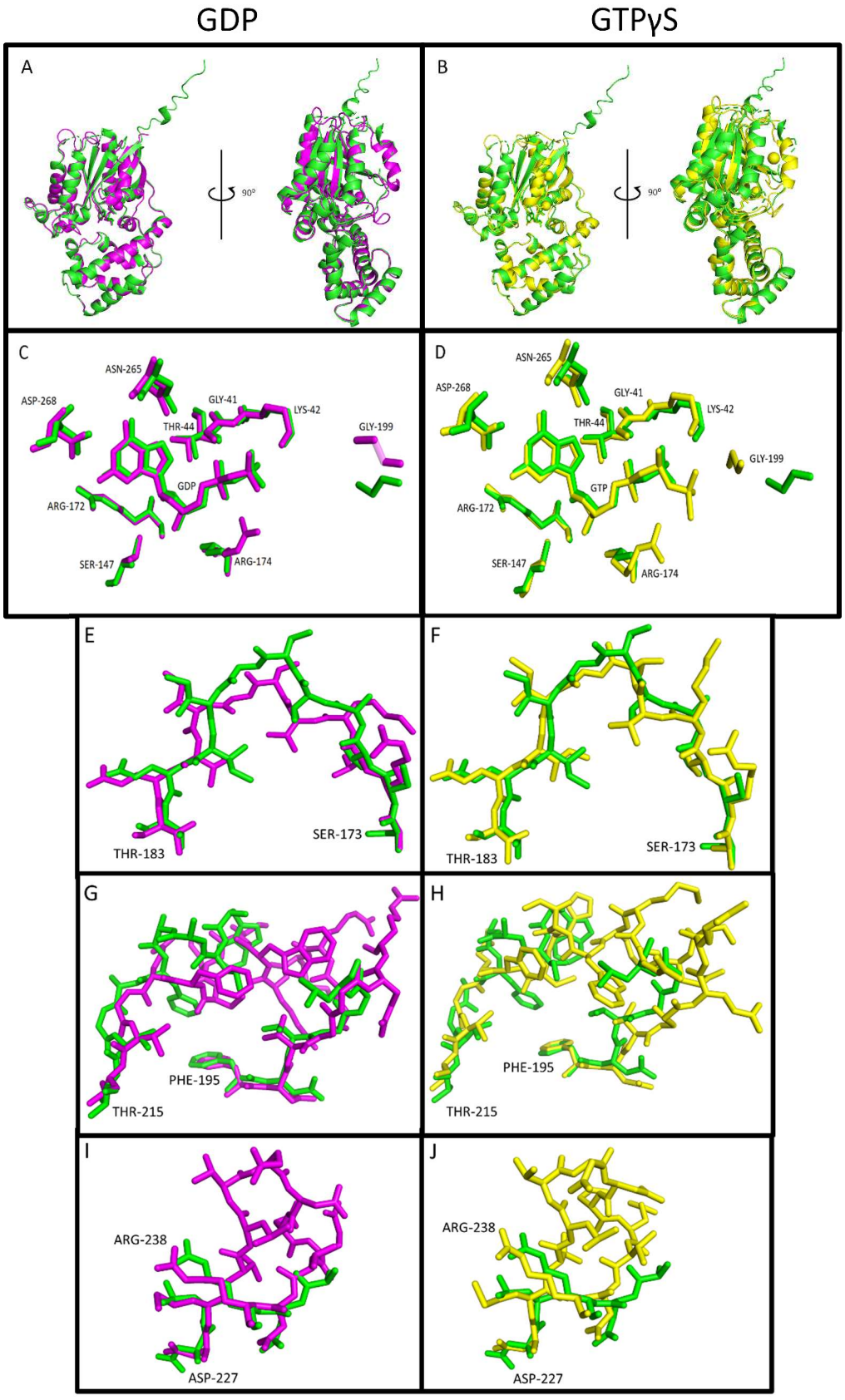
GDP
GTPγS
A
B
90°
90°
C
D
ASN-265
ASP-268
GLY-41
LYS-42
THR-44
GLY-199
GDP
GTP
ARG-172
SER-147
ARG-174
E
F
THR-183
SER-173
G
H
PHE-195
THR-215
I
J
ARG-238
ASP-227

Figure 6: Crystal structure of α_T* SFD QLRC C210S overlapped with 1TND and 1TND. The crystal structure of α_T* SFD QLRC C210S (green) was aligned with the GDP-bound 1TAG structure (purple) and also the 1TND GTPγS 1TND structure (yellow). A, B show the overall structure of α_T* SFD QLRC C210S aligned to either 1TAG or 1TND, respectively. The view was rotated 90 degrees to help visualize of the structure. C, D alignment of α_T* SFD QLRC C210S to either 1TAG or 1TND viewing the guanosine nucleotide binding pocket. Residues and their sequence numbers have been labelled. Note that residue 174 has been mutated from arginine to cysteine in the α_T* SFD QLRC C210S structure and is not labeled. An extra phosphate group can be seen in D which is the γ phosphate of GTPγS. E, F alignment viewing the Switch I region. G, H alignment viewing the Switch II region. I, J alignment viewing the Switch III region. Switch II and III for α_T* SFD QLRC C210S (green) have unmodelled regions due to weak electron density and have missing residues. Each end of the Switch regions are labelled to help identify polarity.

DISCUSSION

This work is important because we can use this active α_T subunit to study its interactions with PDE. By understanding how transducin activates PDE, not only will we better understand the phototransduction signaling pathway but also the other closely related GPCR pathways. GPCRs and their associated proteins in signal transduction present a vast opportunity to develop medicines to treat diseases where these signaling pathways become disrupted. This study aims to further our understanding of G proteins so that we can develop treatments for when aberrant signaling arises as seen in cancer[26].

In this work we crystallized an active form of α_T to see how this chimera activates its effector, PDE. We solved structures of a chimeric α_T subunit mutated to α_T* SFD and then a constitutively active form, α_T* SFD QLRC, which were expressed in *E. coli*. To understand more about G protein signaling, we first used site directed mutagenesis to identify critical residues for GTP hydrolysis. Previous studies by Hargrave *et al.* identified that α_T Chi8 can be expressed in a bacterial system and provided a starting point for further studies. However, α_T Chi8 could not activate its effector protein, PDE. Further mutagenesis by Majumdar *et al.* showed α_T Chi8 HN was able to restore partial effector activity[51]. To restore full effector activity, Milano *et al* 2018, showed that a critical phenylalanine residue within α_T Chi8 HN SFD (α_T* SFD) was necessary to fully restore effector activity. We have extended the story by creating a new α_T mutant which is constitutively active and stimulates PDE despite the absence of rhodopsin.

Generation of this mutant can help us better understand the mechanism by which G proteins activate effector proteins.

Originally, we grew crystals of α_T* SFD in hopes of determining the crystal structure of the active conformation. In doing so, we could compare the chimeric structure to retinal transducin to learn how the critical phenylalanine residue confers maximum PDE activation. However, these crystals diffracted weakly (>3.0 Å) and yielded the inactive GDP-bound state. In crystallography, it is important to obtain the highest resolution structure because higher resolution structures have more resolved electron density. As an example, aromatic structures of low resolution structures look like flat discs. However, in high resolution structures, the electron density is much more refined and now resembles a flat disc with a circular hole in the center. Higher resolution structures better resemble the true three dimensional shape of the protein and greatly facilitate modelling. In higher resolution structures, the electron density reveals specific atomic interactions. For example, higher resolution structures of G proteins can reveal the atoms within the protein that interact with atoms of guanosine. On the contrary, lower resolution structures have less refined electron density and may only show the residues which interact with guanosine and not the individual atoms involved. The ultimate resolution is limited by the wavelength of the X-ray beam used. An X-ray beam is on the same order of length as atomic bonds and interacts with the electrons which form these bonds. Therefore, the maximum resolution using this technique is ~1.0 Å.

To help create an active state crystal structure, the α_T* SFD QLRC mutant was made. It is well known that the Q200L mutation replaces the binding of a glutamate

residue, which normally binds to the γ phosphate of GTP, to a rather inert leucine which helps reduce the GTPase activity. The R174C mutation replaces the arginine finger residue which is analogous to arginine fingers found in GTPase-accelerating proteins (GAPs). Normally, GAPs bind to GTP within activated G_α subunits using an arginine finger and stimulate the G protein's intrinsic GTP hydrolytic activity. By mutating arginine to cysteine, the GTPase activity of α_T was reduced. The α_T* SFD QLRC protein was fully able to stimulate PDE without the need for GTP/GDP exchange (Figure 4). These mutations created a constitutively active form of α_T of which we hoped to solve the crystal structure. Despite these hopes, the crystal structure revealed GDP instead of GTP was bound.

In a further effort to crystallize the α_T* SFD QLRC mutant bound to GTP, inspiration from literature has provided some insight[51]. A recent paper by Hu et. al 2018, crystallizes a G_αS subunit to 1.7 Å. In that study the researchers mutate residue 201 from arginine to cysteine. The researchers claim that this mutation decreases the GTP hydrolysis rate and may change the protein conformation to affect Mg^{2+} and nucleotide properties and promote crystallization of the GTP-bound state (similar to our R174C). The researchers explain a second mutation of residue 237, from serine to cysteine, was necessary to crystallize G_αS and improve diffraction to 1.7 Å. To identify the corresponding residues within α_T, the G_αS sequence was aligned with α_T and the corresponding residue of α_T was mutated to match the mutation in G_αS. One of the two mutations, R1741C, was already present in the α_T* SFD QLRC construct. Using the sequence alignment, the second residue in α_T* SFD QLRC, 210, was mutated from serine to cysteine. The resulting α_T* SFD QLRC C210S mutant was created in hopes of

obtaining a GTP-bound structure. This mutant protein was expressed, purified, and crystallized.

Crystals diffracted to about 2.8 Å but interestingly still contained GDP in the crystal structure. This result is intriguing because α_T was crystallized using GTPγS, a GTP analog that is hydrolyzed very slowly. Perhaps when the mutant protein is expressed in *E. coli* a fraction of purified mutant protein is bound to GDP. Perhaps the crystallization conditions select for the minor GDP-bound state while the GTPγS-bound state remains in solution or precipitates as seen in Figure 5A. Concerning the structure of the GDP-bound state, the α_T* SFD QLRC C210S mutant shows similarities in global alignment and guanosine binding to both the GDP-bound and GTP-bound structures (Figure 6).

Next, we compared the switch regions of α_T* SFD QLRC C210S to each native structure. Switch I had high electron density and was modelled well unlike Switch II and III. The structure of Switch I looks similar to both GDP and GTPγS crystals and cannot be characterized as either in active or inactive conformation. Low electron density of both Switch II and III made it difficult to determine which conformation the α_T* SFD QLRC C210S mutant more closely resembles. Due to the low electron density, the structure cannot be modeled in these regions. Amino acids excluded from Switch II include: 201-206. Amino acids excluded from Switch III include: 229-235. However, as evident by the weak electron density in Switch II and III, the mutant appears to be in a transition state between GDP and GTP bound states. Perhaps the protein transitions between active and inactive states and therefore results in flexible regions (Figure 4). It

is known that the Switch regions move when transducin binds GTP and may explain these results. Normally, the Switch regions are structured in retinal α when bound to GDP or GTP as seen in Figure 6. Therefore, GDP may not be insufficient to stabilize the active conformation. Further work is needed to obtain crystals which diffract well and have structured Switch II and III regions.

Before the α_T chimera was developed for expression in *E. coli*, only retinal structures existed. In these structures, and other Gα proteins, the first 25 residues were cleaved to promote crystallization and diffraction. Cleaving these C-terminal residues removes lipid-anchoring hydrophobic residues. Additionally, these residues are modified with a 14-carbon saturated fatty acid chain (myristoylation) which also tethers the α subunit to the membrane and rhodopsin. By removing these residues, α_T becomes more soluble and promotes crystallization. In the α_T* SFD QLRC C210S structure, the first 25 residues have not been cleaved (Figure 5) while both the GDP and GTP bound structures have been cleaved. (Figures 6A and 6B). Recent experiments aim to remove the first 25 residues to improve diffraction. Using polymerase chain reaction, (PCR), a SUMO or TEV sequence can be inserted between residues 25 and 26 of α_T* SFD QLRC C210S. These certain protein sequences can be specifically recognized and cleaved by their respective proteases. Both SUMO and TEV cleavage techniques are currently being implemented to remove the first 25 residues. Since the native structures could not be mutated the endoprotease, LysC, was employed to cleave polypeptides on the C-terminal side of lysines to remove the first 25 residues of α subunits. As one caveat, LysC digestion can be over incubated and degrade protein beyond the desired cleavage length. Using SUMO and TEV proteases instead of LysC provides more

control and may yield higher diffracting crystals. Crystal screens for α_T* SFD QLRC C210S SUMO or TEV mutants have been set up and new conditions are being searched for.

Another step to improve the structure is to express these mutant proteins in insect cells. Insect cells are eukaryotic and are currently used in the lab to purify other proteins such as rhodopsin. Insect cells have the advantage of post-translationally modifying proteins unlike prokaryotic bacterial cells. Perhaps expression in insect cells may increase protein yields and improve diffraction. If so, the structure may contain GTP and have structured Switch II and Switch III regions. In doing so, we can observe how the structure of the constitutively active α_T* SFD QLRC C210S mutant (the phenylalanine residue in particular) activates PDE. By creating this mutant and solving its crystal structure, we hope to improve G protein research *in vitro.*

REFERENCES

1. Neer, Eva J., and David E. Clapham. "Roles of G protein subunits in transmembrane signalling." Nature 333.6169 (1988): 129.
2. Palczewski, Krzysztof. "G protein–coupled receptor rhodopsin." *Annu. Rev. Biochem.* 75 (2006): 743-767.
3. Jastrzebska, Beata. "Rhodopsin."
4. Fredriksson, Robert, et al. "The G-protein-coupled receptors in the human genome form five main families. Phylogenetic analysis, paralogon groups, and fingerprints." *Molecular pharmacology* 63.6 (2003): 1256-1272.
5. Bjarnadóttir, Thóra K., et al. "Comprehensive repertoire and phylogenetic analysis of the G protein-coupled receptors in human and mouse." *Genomics* 88.3 (2006): 263-273.
6. Santos, Rita, et al. "A comprehensive map of molecular drug targets." *Nature reviews Drug discovery* 16.1 (2017): 19.
7. Bowmaker, James K., and HJk Dartnall. "Visual pigments of rods and cones in a human retina." The Journal of physiology 298.1 (1980): 501-511.
8. Palczewski, Krzysztof, et al. "Crystal structure of rhodopsin: AG protein-coupled receptor." *science* 289.5480 (2000): 739-745.
9. Okada, Tetsuji, et al. "The retinal conformation and its environment in rhodopsin in light of a new 2.2 Å crystal structure." *Journal of molecular biology* 342.2 (2004): 571-583.

10. Scheerer, Patrick, et al. "Crystal structure of opsin in its G-protein-interacting conformation." Nature 455.7212 (2008): 497.
11. Ridge, Kevin D., and Krzysztof Palczewski. "Visual rhodopsin sees the light: structure and mechanism of G protein signaling." *Journal of Biological Chemistry* 282.13 (2007): 9297-9301.
12. Rasmussen, Søren GF, et al. "Crystal structure of the β 2 adrenergic receptor–Gs protein complex." *Nature* 477.7366 (2011): 549.
13. Chung, Ka Young, et al. "Conformational changes in the G protein Gs induced by the β 2 adrenergic receptor." *Nature*477.7366 (2011): 611.
14. DeVree, Brian T., et al. "Allosteric coupling from G protein to the agonist-binding pocket in GPCRs." *Nature* 535.7610 (2016): 182.
15. Draper-Joyce, Christopher J., et al. "Structure of the adenosine-bound human adenosine A 1 receptor–G i complex." *Nature* 558.7711 (2018): 559.
16. Gao, Yang, et al. "Purification of the Rhodopsin–Transducin Complex for Structural Studies." *Protein Lipidation*. Humana, New York, NY, 2019. 307-315.
17. Preininger, Anita M., Jens Meiler, and Heidi E. Hamm. "Conformational flexibility and structural dynamics in GPCR-mediated G protein activation: a perspective." *Journal of molecular biology* 425.13 (2013): 2288-2298.
18. Manglik, Aashish, et al. "Structural insights into the dynamic process of β2-adrenergic receptor signaling." *Cell* 161.5 (2015): 1101-1111.
19. Deupi, Xavier, et al. "Stabilized G protein binding site in the structure of constitutively active metarhodopsin-II." *Proceedings of the National Academy of Sciences* 109.1 (2012): 119-124.

20. Veprintsev, Dmitry B., and M. Madan Babu. "Universal allosteric mechanism for Ga activation by GPCRs."
21. Dror, Ron O., et al. "Structural basis for nucleotide exchange in heterotrimeric G proteins." *Science* 348.6241 (2015): 1361-1365.
22. Dohlman, Henrik G., and Jeremy Thorner. "RGS proteins and signaling by heterotrimeric G proteins." Journal of Biological Chemistry 272.7 (1997): 3871-3874.
23. Downes, G. B., and N. Gautam. "The G protein subunit gene families." *Genomics* 62.3 (1999): 544-552.
24. Li, Fangxia, Márcio De Godoy, and Satish Rattan. "Role of adenylate and guanylate cyclases in β1-, β2-, and β3-adrenoceptor-mediated relaxation of internal anal sphincter smooth muscle." *Journal of Pharmacology and Experimental Therapeutics* 308.3 (2004): 1111-1120.
25. Preininger, Anita M., and Heidi E. Hamm. "G protein signaling: insights from new structures." *Sci. STKE* 2004.218 (2004): re3-re3.
26. O'hayre, Morgan, et al. "The emerging mutational landscape of G proteins and G-protein-coupled receptors in cancer." *Nature Reviews Cancer* 13.6 (2013): 412.
27. Traut, Thomas W. "Physiological concentrations of purines and pyrimidines." Molecular and cellular biochemistry 140.1 (1994): 1-22.
28. O'Halloran, DAMIEN M., DAVID A. Fitzpatrick, and A. M. Burnell. "The chemosensory system of Caenorhabditis elegans and other nematodes." Chemical ecology: from gene to ecosystem 16 (2006): 71.

29. Wall, Mark A., et al. "The structure of the G protein heterotrimer Giα1β1γ2." *Cell* 83.6 (1995): 1047-1058.
30. Cherfils, Jacqueline, and Marc Chabre. "Activation of G-protein Gα subunits by receptors through Gα–Gβ and Gα–Gγ interactions." *Trends in biochemical sciences* 28.1 (2003): 13-17.
31. Sondek, John, et al. "Crystal structure of a GA protein βγdimer at 2.1 Å resolution." *Nature* 379.6563 (1996): 369.
32. Simon, Melvin I., Michael P. Strathmann, and Narasimhan Gautam. "Diversity of G proteins in signal transduction." *Science* 252.5007 (1991): 802-808.
33. Noel, Joseph P., Heidi E. Hamm, and Paul B. Sigler. "The 2.2 Å crystal structure of transducin-α complexed with GTPγS." *Nature* 366.6456 (1993): 654.
34. Lambright, David G., et al. "The 2.0 Å crystal structure of a heterotrimeric G protein." *Nature* 379.6563 (1996): 311.
35. Lambright, David G., et al. "Structural determinants for activation of the α-subunit of a heterotrimeric G protein." Nature 369.6482 (1994): 621.
36. Slep, Kevin C., et al. "Structural determinants for regulation of phosphodiesterase by a G protein at 2.0 Å." *Nature* 409.6823 (2001): 1071.
37. Zhang, Zhixian, et al. "Domain organization and conformational plasticity of the G protein effector, PDE6." *Journal of Biological Chemistry* 290.20 (2015): 12833-12843.
38. Arshavsky, Vadim Y., et al. "Regulation of transducin GTPase activity in bovine rod outer segments." *Journal of Biological Chemistry* 269.31 (1994): 19882-19887.

39. Skiba, Nikolai P., Hyunsu Bae, and Heidi E. Hamm. "Mapping of effector binding sites of transducin α-subunit using Gαt/Gαil chimeras." *Journal of Biological Chemistry* 271.1 (1996): 413-424.
40. Milano, Shawn K., et al. "Gain-of-function screen of α-transducin identifies an essential phenylalanine residue necessary for full effector activation." *Journal of Biological Chemistry* 293.46 (2018): 17941-17952.
41. Tesmer, John JG, et al. "Crystal structure of the catalytic domains of adenylyl cyclase in a complex with Gsα· GTPγS." *Science* 278.5345 (1997): 1907-1916.
42. Sadana, Rachna, and Carmen W. Dessauer. "Physiological roles for G protein-regulated adenylyl cyclase isoforms: insights from knockout and overexpression studies." *Neurosignals* 17.1 (2009): 5-22.
43. Dessauer, Carmen W. "Adenylyl cyclase–A-kinase anchoring protein complexes: the next dimension in cAMP signaling." Molecular pharmacology 76.5 (2009): 935-941.
44. Z. Otwinowski and W. Minor, " Processing of X-ray Diffraction Data Collected in Oscillation Mode ", Methods in Enzymology, Volume 276: Macromolecular Crystallography, part A, p.307-326, 1997,C.W. Carter, Jr. & R. M. Sweet, Eds., Academic Press (New York)
45. PHENIX: a comprehensive Python-based system for macromolecular structure solution. P.D. Adams, P.V. Afonine, G. Bunkoczi, V.B. Chen, I.W. Davis, N. Echols, J.J. Headd, L.W. Hung, G.J. Kapral, R.W. Grosse-Kunstleve, A.J. McCoy, N.W. Moriarty, R. Oeffner, R.J. Read, D.C. Richardson, J.S. Richardson, T.C. Terwilliger, and P.H. Zwart. Acta Cryst. D66, 213-221 (2010).

46. Fawzi, Ahmad B., and John K. Northup. "Guanine nucleotide binding characteristics of transducin: essential role of rhodopsin for rapid exchange of guanine nucleotides." Biochemistry 29.15 (1990): 3804-3812.
47. Min, K. Christopher, Stephen A. Gravina, and Thomas P. Sakmar. "Reconstitution of the vertebrate visual cascade using recombinant heterotrimeric transducin purified from Sf9 cells." Protein expression and purification 20.3 (2000): 514-526.
48. Matte, Suzanne L., Thomas M. Laue, and Rick H. Cote. "Characterization of conformational changes and protein-protein interactions of rod photoreceptor phosphodiesterase (PDE6)." *Journal of Biological Chemistry* 287.24 (2012): 20111-20121.
49. Majumdar, Sharmistha, Sekar Ramachandran, and Richard A. Cerione. "New insights into the role of conserved, essential residues in the GTP binding/GTP hydrolytic cycle of large G proteins." *Journal of Biological Chemistry* 281.14 (2006): 9219-9226.
50. The PyMOL Molecular Graphics System, Version 1.2r3pre, Schrödinger, LLC.
51. Majumdar, Sharmistha, Sekar Ramachandran, and Richard A. Cerione. "Perturbing the Linker Regions of the α-Subunit of Transducin A NEW CLASS OF CONSTITUTIVELY ACTIVE GTP-BINDING PROTEINS." *Journal of Biological Chemistry*279.38 (2004): 40137-40145.
52. Hu, Qi, and Kevan M. Shokat. "Disease-causing mutations in the G protein Gαs subvert the roles of GDP and GTP." *Cell*173.5 (2018): 1254-1264.

53. Paul Emsley and Bernhard Lohkamp and William G. Scott and Kevin Cowtan. “Features and Development of Coot.” Acta Crystallographica Section D - Biological Crystallography, 2010, 66, 486-501
54. Kimple, Adam J., et al. "Regulators of G-protein signaling and their Gα substrates: promises and challenges in their use as drug discovery targets." *Pharmacological reviews* 63.3 (2011): 728-749.
55. Giese, Arthur C., ed. Photophysiology: General Principles; Action of Light on Plants. Elsevier, 2013.
56. Zhou, X. Edward, Karsten Melcher, and H. Eric Xu. "Structure and activation of rhodopsin." *Acta pharmacologica Sinica* 33.3 (2012): 291.
57. Hargrave, Paul A., Heidi E. Hamm, and K. P. Hofmann. "Interaction of rhodopsin with the G-protein, transducin." *BioEssays* 15.1 (1993): 43-50.
58. Standfuss, Jörg, et al. "The structural basis of agonist-induced activation in constitutively active rhodopsin." *Nature* 471.7340 (2011): 656.
59. Sondek, John, et al. "GTPase mechanism of Gproteins from the 1.7-Å crystal structure of transducin α-GDP AIF− 4." *Nature* 372.6503 (1994): 276.
60. Neves, Susana R., Prahlad T. Ram, and Ravi Iyengar. "G protein pathways." Science 296.5573 (2002): 1636-1639.
61. Yang Gao, Hongli Hu, Sekar Ramachandran, Jon W. Erickson, Richard A. Cerione, Georgios Skiniotis. “Structures of the Rhodopsin-Transducin Complex: Insights into G-Protein Activation.” Molecular Cell 75, 1-10 (2019)